energies

MDPI

Article

Effect of AC Pre-Charging of Epoxy Insulator on Flashover Properties in Eco-Friendly Binary Gas Mixtures

Jian Guan [1], Guohui Han [1], Qifeng Shang [2,*], Xiaohu Qi [1], Zhiying Wang [1] and Yu Gao [2]

[1] Henan Pinggao Electric Co., Ltd., No. 22, Nanhuan East Road, Pingdingshan 467000, China
[2] School of Electrical and Information Engineering, Tianjin University, 92 Weijin Road, Tianjin 300072, China
* Correspondence: sqifeng@tju.edu.cn

Abstract

Metal particles and surface charge accumulation are considered the key factors that could trigger unexpected flashovers of insulators equipped in gas-insulated switchgear (GIS). In eco-friendly gases, the flashover properties and the synergistic effect of the surface charge and the metal particle on flashover remain unclear. This study investigates the flashover properties of down-scaled 252 kV GIS basin-type epoxy insulators with metal particles in C_4F_7N/CO_2 mixtures, with and without AC pre-charging. Tests considered various particle adherence locations and a particle-free control group. The results indicated that metal particles at the high-voltage (HV) electrode or middle area reduce flashover voltage, with the HV electrode and concave surface being most critical. Surface charges, induced by pre-charging and metal particle attachment, interact synergistically with the metal particle during the flashover process, increasing the flashover voltage and redirecting arcs away from them. Such findings enhance understanding of flashover mechanisms in eco-friendly gas-insulated systems and inform insulator design.

Keywords: gas-insulated switchgear; C_4F_7N/CO_2; flashover; surface charge; metal particle

check for updates

Academic Editor: Carlos Miguel Costa

Received: 29 August 2025
Revised: 17 October 2025
Accepted: 23 October 2025
Published: 25 October 2025

Citation: Guan, J.; Han, G.; Shang, Q.; Qi, X.; Wang, Z.; Gao, Y. Effect of AC Pre-Charging of Epoxy Insulator on Flashover Properties in Eco-Friendly Binary Gas Mixtures. *Energies* **2025**, *18*, 5612. https://doi.org/10.3390/en18215612

Copyright: © 2025 by the authors. Licensee MDPI, Basel, Switzerland. This article is an open access article distributed under the terms and conditions of the Creative Commons Attribution (CC BY) license (https://creativecommons.org/licenses/by/4.0/).

1. Introduction

Gas-insulated switchgear (GIS) has gained widespread application in power systems due to its excellent properties in reliability, land occupation, and maintenance requirements [1–3]. In recent years, incidents of insulation failure in GIS have occurred frequently, posing severe threats to the safety and reliability of the power grid [4]. Insulator is one of the most vital insulating components in GIS, separating gas chambers, supporting the central conductor, and most importantly, isolating the high voltage (HV) from the ground (GND) [5]. The insulation properties at the gas–solid interface represent the weak point constraining the overall insulation performance of GIS. During the production, transportation, installation, and operation of GIS, metal particles are inevitably generated and may fall or be absorbed onto the surface of the insulators, distorting the electric field and leading to flashover failures. Surface charge accumulation, whose generation is closely related to metal particles under AC voltage, is also an important trigger to flashover [6]. Therefore, understanding the effect of pre-charging on flashover properties has significant importance in revealing the mechanism of synergistic effects of metal particle and surface charge and benefiting the power system.

In recent decades, scholars across the world have conducted extensive research on the charge accumulation characteristics and surface flashover properties of different solid insulation materials. X. Jun et al. [7] investigated the effect of surface charge on the impulse

flashover of cylindrical Polytetrafluoroethylene (PTFE) insulators in SF_6 at 1 bar, pointing out that the 50% impulse flashover voltage was reduced by 25% when negative charge was presented on the surface, while the flashover voltage increased by 21% when positive charge was presented. A. Winter et al. [8] reported that with negative surface charge deposited, the flashover voltage of a PTFE plate specimen in 100 kPa SF_6 was reduced by 20% for positive DC and by 25% for AC voltage. Y. Liu et al. [9] deposited positive charges on an Al_2O_3-filled epoxy resin plate in 0.1 MPa SF_6, finding that when the charge density is from 0 to 1.4 nC/mm^2, the negative flashover voltage reduced by 7%, and the positive flashover voltage increased by 15%. Q. Xie et al. [10] revealed that the surface charge on the polymer surface would enhance the electric field and promote the DC flashover. Overall, plentiful research has been performed to investigate the surface-charge-affected flashover properties in SF_6 atmospheres; charges accumulated on the surface will distort the electric field, but the mechanism of its influence on AC flashover is still unclear.

With a comparable dielectric strength and relatively low global warming potential (GWP), eco-friendly gases, for example, the C_4F_7N/CO_2 mixtures are regarded as promising substitutes for SF_6. Y. Kieffel et al. [11] reported that compared with SF_6, the $4\%C_4F_7N/96\%CO_2$ mixture could reduce the GWP up to 98% while still keeping a liquefaction temperature of lower than −25 °C and about 70% of the dielectric strength of SF_6. Z. Li et al. [12,13] indicated that the addition of minor amounts of C_4F_7N to CO_2 enhances the surface flashover voltage, with further increases observed as both the gas pressure and C_4F_7N proportion rise. Specifically, the flashover voltage of insulators in a 9% C_4F_7N/91% CO_2 mixture at 0.6 MPa is comparable to that in SF_6 at 0.5 MPa. Previous research has generally focused on the surface-charge-affected flashover properties in SF_6-related atmospheres, and the charges are usually deposited manually. Under AC voltage, surface charge accumulation on insulators in eco-friendly gases is intricate, especially with metal particles adhered. In eco-friendly gases, the flashover properties and the synergistic effect of the surface charge and the metal particle on flashover remain unclear.

In this paper, the flashover properties with and without pre-charging on down-scaled 252 kV GIS basin-type insulator models attached with metal particles in C_4F_7N/CO_2 mixtures were investigated. Multiple adherence areas were considered, and an instance free of metal particles was set up as a control group. The results indicated that the metal particle will decrease the flashover voltage when attached to the HV electrode and the middle area of the insulator; the attachment to the HV electrode and the concave surface is more dangerous. Surface charge induced by pre-charging will act synergistically with the metal particle during the flashover process, increasing the flashover voltage and driving the arc away.

2. Materials and Methods

2.1. Sample and Experiment Platform

Down-scaled basin-type insulators, whose prototype could be utilized in 252 kV AC GIS systems, were employed as the test samples in this study. The epoxy composite comprises epoxy resin and micro-scale Al_2O_3 filler at a 1:3 mass ratio; the central conductor and the flange are made of aluminum. The insulator samples were produced by Taikai Group Co. Ltd., Taian, China, and the diagram of the sample is shown in Figure 1.

As demonstrated in Figure 2, a sealed multifunctional experimental platform was employed to charge the sample and perform subsequent experiments. The HV electrode served to charge the insulator, positioned at the base of the chamber. Valves and a pressure gauge facilitated the establishment of specific gas environments during the procedures. The pressure gauge exhibited an accuracy of 0.0001 MPa, enabling the precise preparation of gas mixtures in desired ratios. Surface potential measurements were performed using

a Kelvin probe (3455ET, Trek, New York, NY, USA) connected with an electrostatic voltmeter (P0865, Trek). The measurement apparatus incorporated a linear shifting platform and a rotational platform (MTS and MRS Series, Becic, Beijing, China), with comprehensive details available in our prior work [14].

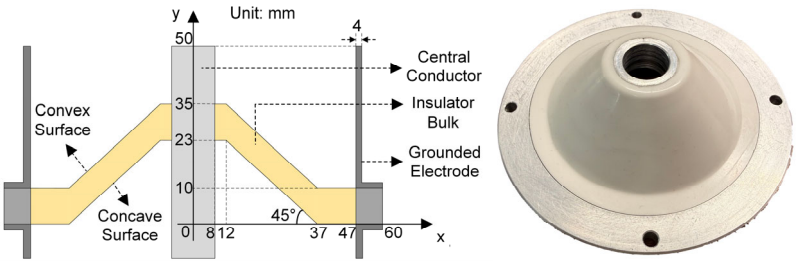


Figure 1. The diagram and the photograph of the insulator sample.

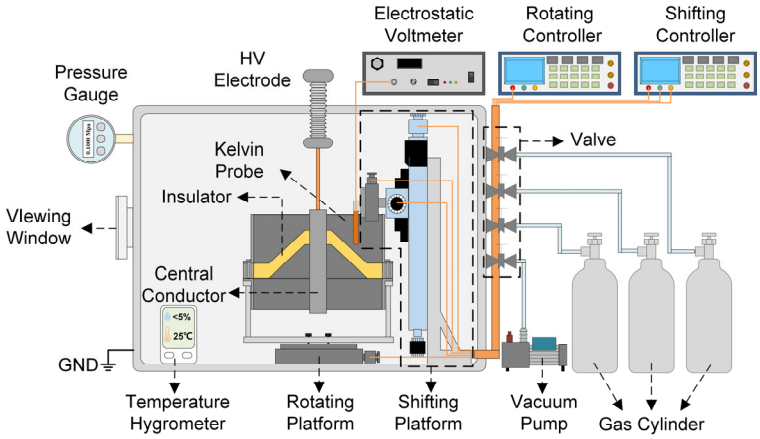


Figure 2. Multifunctional experimental platform.

In the measurement of the surface potential, the insulator turntable and data acquisition card were activated simultaneously. The turntable rotates at an angular velocity of 20°/s, while the acquisition card scans the sampling circumference corresponding to the initial sampling point at a fixed frequency. After the insulator completes a 360° rotation, the insulator rotation platform stops. Simultaneously, the *X*-axis, *Y*-axis, and probe rotation platform are activated to move the probe to the next sampling point along the insulator's radial direction. Upon reaching the next sampling point and adjusting the angle, the insulator rotation platform and data acquisition card are synchronously activated via the program to scan the corresponding sampling circle. This cycle repeats until the probe completes scanning all sampling circles. Finally, the probe is returned to the beginning position, and the electrometer is turned off, concluding the surface potential scanning measurement of the insulator. A total of 72 sampling points are arranged in a single circle, and 9 circles are distributed uniformly on the surface in total. A total of 648 surface potential data points were acquired over a duration of 252 s, and the charge density was derived employing an inversion algorithm based on COMSOL Multiphysics 6.2 [14].

The inversion algorithm employs a simulated charge method. The approach involves establishing the relationship between the charge density σ at each point on the surface and the measured surface potential φ through the transfer function matrix H:

$$\varphi = H\sigma \quad (1)$$

The matrix H is computed using COMSOL Multiphysics. First, a 3D model of the insulator and electrodes is created in COMSOL, with a mesh identical to the sampling

grid. After meshing, the grid is numbered: the outermost mesh is designated as number 1, and subsequent meshes are numbered counterclockwise around each layer. Using the COMSOL Electrostatic Field Module, assign a unit surface charge density of 1 pC/mm^2 to mesh 1. Employ the finite element method to calculate the average surface charge on mesh 1 and the induced charge on each mesh, considering both the ground electrode and the central electrode grounded. Then, the surface charge density of grid 1 is reset to zero. The next adjacent grid is selected, and the COMSOL Electrostatic Field Module is again used to assign a unit surface charge density to this grid. The average potential values across all grids are calculated. This process is repeated for all 648 grids to form the H matrix. The surface charge density is then calculated through function (1).

2.2. Procedure

Prior to the experiment, all samples were dried at 60 °C for 12 h to remove the absorbed moisture and wiped with absolute ethanol to remove the residual surface charge. Due to the fact that the shape of the metal particles observed in GIS is more likely to be linear and needle-like [15], aluminum wire was chosen in this experiment. To focus on the effect of metal particles on surface charge distribution and flashover properties, the measurements of the particles were 5 mm in length and 0.5 mm in width, which would sufficiently distort the electric field and strengthen the gas-side ionization, while a larger size would also facilitate the experiment. As shown in Figure 3, the metal particle was adhered to multiple areas on the surface of the sample, including the HV electrode area, the middle (MID) area, and the grounded electrode area on both the convex surface and the concave surface. Only one metal particle was adhered to the sample in each test, and an instance of no metal particles was also set up for comparison.

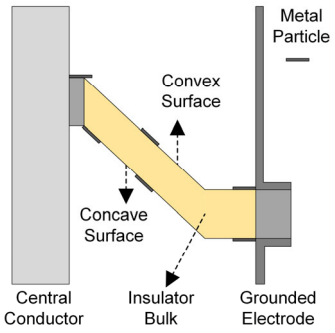


Figure 3. Positions of the metal particle.

The experiments were performed at room temperature, and the parameters of the C_4F_7N/CO_2 mixture were 6%/94% in proportion and 0.1 MPa in pressure. A coaxial electrode configuration was employed to replicate the authentic electric field distribution within a full-scale 252 kV GIS, with the AC voltage amplitude established at 40 kV. The experiment was generally divided into two parts: flashover without pre-charging and flashover with pre-charging. In the first part, the voltage applied to the central electrode rose at a rate of 1 kV/s until the flashover occurred. In the second part, the voltage applied to the central electrode rose at the same rate to 40 kV at first. After being charged for 5 min, the voltage was cut off, and the surface potential was measured. Because the measurement was performed within 5 min, the surface charge density was regarded as unchanged. Then, the voltage was applied again at the same rate until the flashover occurred. As indicated in our prior investigation [16], following the application of HVAC for durations of 2, 5, 30, and 60 min, the charge distribution profiles exhibited negligible variations, with charge accumulation approaching a state of dynamic equilibrium. Consequently, the charging duration in this study was fixed at 5 min to achieve substantial charge buildup while en-

abling efficient replication of experimental trials. The samples were replaced after each flashover. Each test was repeated at least 5 times, and their average value was treated as the flashover voltage, as presented and discussed in this paper.

3. Results

3.1. Effect of Metal Particle Position on Flashover Voltage

Figure 4 displays the average flashover voltage of the sample without being charged. The results show a significant decrease in the flashover voltage when a metal particle is adhered to the HV electrode on both surfaces of the sample. In the control group, which is free of metal particles, the flashover voltage is 55.3 kV. With a metal particle adhered to the HV electrode on the convex surface and the concave surface of the sample; however, the flashover voltage drops by 19%, to 44.8 kV and 45.4 kV, respectively. When attached to the middle area of the sample, the effect of the metal particle on the flashover voltage turns out to be different on both sides. On the convex side, little decrease in the flashover voltage is observed, dropping only by 4%, to 53.2 kV, while on the concave side, the flashover voltage still drops by 10%, to 49.5 kV. When the metal particle is attached to the grounded electrode, the flashover voltage is 53.5 kV and 55.9 kV, respectively. To sum up, without pre-charging, the metal particle will decrease the flashover voltage when attached to the HV electrode and the middle area of the insulator. The attachment of metal particles to the HV electrode of the insulator has a more pronounced effect on the flashover voltage than the middle area, and the attachment to the concave surface is more dangerous than the convex surface.

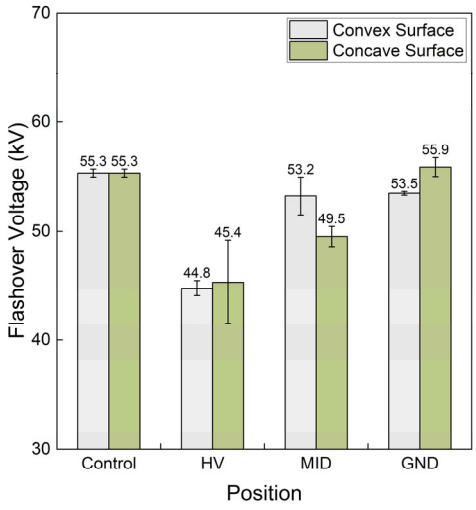


Figure 4. Average flashover voltage without pre-charging.

3.2. Effect of Pre-Charging on Flashover Voltage

Figures 5 and 6 display the average flashover voltage of the sample with and without pre-charging. It can be seen that, after a pre-charge procedure of 5 min, the flashover voltages of all instances, except the control group and the GND group on the concave surface, increase. A most significant effect of pre-charging on the flashover voltage is observed when the metal particle is attached to the HV electrode on both surfaces. The flashover voltage increased by 10.4 kV, to 55.2 kV, on the convex side and by 9.5 kV, to 54.9 kV, on the concave side. When the metal particle is adhered to the middle area of the surface, the flashover voltage increased by 3.1 kV, to 56.3 kV, on the convex side and by 6.7 kV, to 56.2 kV, on the concave side. When the metal particle is attached to the ground electrode, the flashover voltage increased by 0.9 kV, to 54.4 kV, on the convex side and decreased by 3.0 kV, to 52.9 kV, on the concave side. As for the control group, the effect of pre-charging

is not obvious. The flashover voltages with or without pre-charging are nearly the same, 55.3 kV and 55.1 kV, respectively. To sum up, after a 5 min procedure of pre-charging, the flashover voltage of the sample, adhered with a metal particle, rises to nearly the same level as the instance of no metal particle adhered.

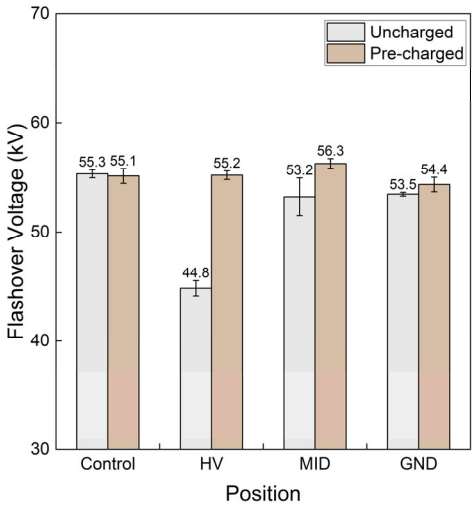


Figure 5. Effect of pre-charging with a metal particle on the convex surface.

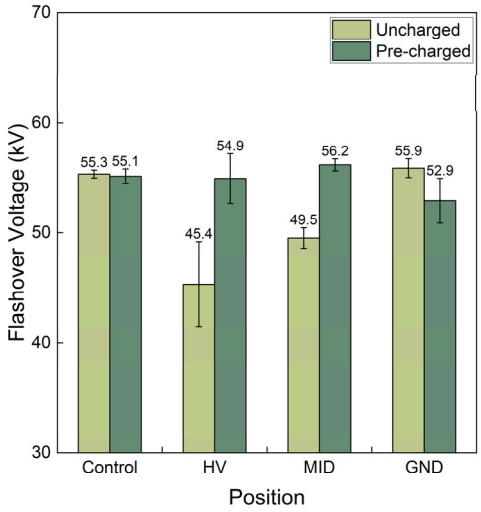


Figure 6. Effect of pre-charging with a metal particle on the concave surface.

3.3. Effect of Surface Charge on Flashover Paths

In the atmosphere of the C_4F_7N/CO_2 mixture, carbonized burnt traces are left on the surface of the sample after the flashover occurs, and flashover paths are only found on the concave surface no matter of whether and where the metal particle is adhered. In the control group, the flashover paths are randomly distributed on the concave surfaces of the samples. In instances of metal particles, however, the distribution of the flashover paths becomes regular. Figure 7 presents the flashover paths of the samples with metal particles adhered to the concave surface. The result indicates that the pre-charging process will drive the flashover arc away from the metal particle. As illustrated in Figure 7a,c,e, when the sample is not charged, the flashover occurs through the metal particles and melts them down. After being charged, however, none of the flashovers occur through the metal particles, as shown in Figure 7b,d,f.

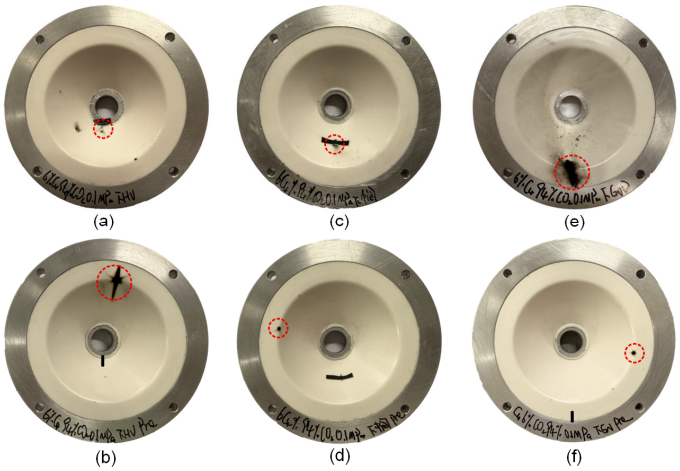


Figure 7. Effect of pre-charging on flashover paths (marked in red circles). The characters on the flange are the description of experimental conditions ("下" means the concave surface, "中间" means MID): (**a**) HV, not charged; (**b**) HV, pre-charged; (**c**) MID, not charged; (**d**) MID, pre-charged; (**e**) GND, not charged; (**f**) GND, pre-charged.

To investigate the outcome of the pre-charging process more specifically, the surface charge distribution on the samples after the pre-charging process is examined. Figure 8 shows the surface charge distribution on the concave surface of the sample with metal particles adhered to the concave surface.

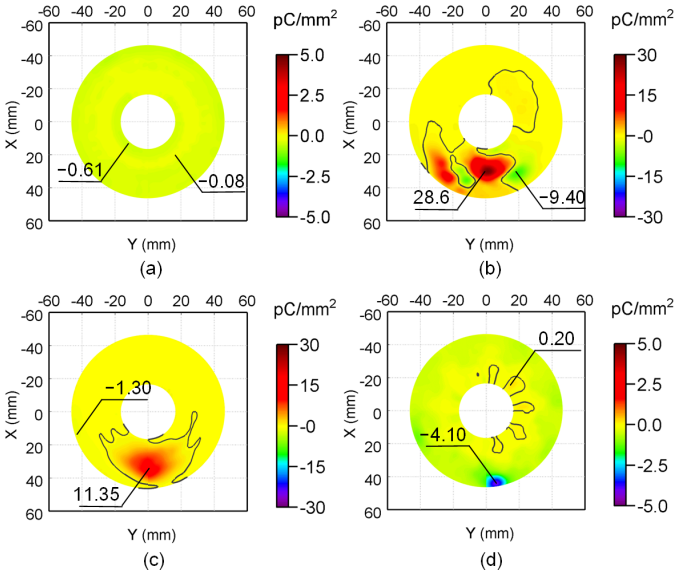


Figure 8. The concave surface charge distribution after pre-charging: (**a**) Control group; (**b**) HV electrode; (**c**) Middle area; (**d**) GND electrode.

In the control group, few surface charges are accumulated. With a metal particle adhered, however, charge spots are induced near the particle. As demonstrated in Figure 8b–d, positive charge spots are detected when the metal particle is adhered to the HV electrode and the middle area of the concave surface, with a maximum charge density of 28.6 pC/mm^2 and 11.35 pC/mm^2 respectively, while negative charge spots are observed when the metal particle is attached to the ground electrode, with a maximum charge density of −4.1 pC/mm^2. The results indicate that compared with the other two positions, the metal particle adhered to the HV electrode triggers the strongest distortion to the electric field, followed by the middle area, and then the grounded electrode. Compared with the flashover paths demonstrated in Figure 7, it is indicated that the surface charge induced

by the metal particle will act synergistically with the metal particle during the flashover process and drive the arc away from itself. To sum up, carbonized burnt traces are left on the concave surface of the sample during the flashover, and the flashover paths are distributed randomly when the metal particle is on the convex surface. When the metal particle is on the concave surface, the flashover occurs through the metal particles, but after pre-charging, the flashover arcs are driven away from the metal particle.

4. Discussion

It is considered that the flashover can be affected by the following three aspects: solid insulation, gas atmosphere, and solid–gas interface [17]. Given the fixed polymer insulation material and the gas atmosphere, the flashover properties affected by surface charges are mainly analyzed from the perspective of the gas–solid interface in this paper. The insulators in this experiment are prepared with epoxy resin and micro-scale Al_2O_3 filler, which will introduce physical and chemical defects on the surface of the insulator. Due to the effects of these defects, charges are easily trapped and accumulated on the surface of the insulator, forming charge spots and affecting flashover properties [18].

When the flashover occurs, arcs develop on the gas–solid interface of the insulator, inducing thermal effects and generating high-speed particles near the channel. With the high temperature of the arc, the epoxy resin is degraded, and the corroded trace is left [19]. The energy of these particles is high enough to break the molecular bonds of the gas and cause the deep decomposition of C_4F_7N, generating solid by-products like carbon [20]. Under the action of airflow and the electric field, the powdered solid by-products were driven to the sample surface and the corroded area, forming black traces.

Metal particles adhered to the insulator will distort the electric field and aggravate the gas side discharge. The normal component of the electric field accelerates the charge accumulation, while the tangential component induces flashover. When the metal particle is attached to the HV electrode and the middle area, like a needle electrode, the local electric field is severely distorted. As shown in Figure 9, when the metal particle is adhered to the middle area, for example, gas side ionization is induced, and the tangential component of the electric field is enhanced. Metal particles connected to the HV electrode have a more severe distorting effect on the electric field. The induction of localized small streamers occurs readily, thereby diminishing the effective surface insulation distance and facilitating the surface flashover. Given the geometric shape of the basin-type insulator, the flashover is difficult to develop along the convex surface because of the electric field distribution and the structural difference. On the concave surface, the flashover is considered to originate from the gas side, with electrons colliding with the insulator surface and developing along the surface to form flashover traces [13]. When adhered to the concave surface, the distorting effect of the metal particle on the concave electric field is stronger than the convex positions. Thus, the flashover voltages of the concave groups are lower than the convex ones, and the HV groups are lower than the middle area groups.

After 5 min of pre-charging, however, the introduction of the surface charge changes the previous situation. Driven by the normal component of the electric field, charges tend to accumulate on the surface of the insulator beneath the metal particle. Charge spots produce a strong electric field and distort the electric field. When the metal particle is adhered to the HV area and the middle area, positive charge spots are accumulated. As shown in Figure 10, during the positive half cycle of the AC voltage, the positive charge spot mitigates the electric field between the metal particle and the central conductor, suppressing the gas side ionization and reducing the free electrons in the local space, which also suppresses the origination of the flashover. In the negative half cycle, although the positive charge spot strengthens the electric field between the metal particle and the central con-

ductor and enhances the gas side ionization, the tangential electric field along the surface of the insulator, however, is mitigated, which suppresses the development of the flashover. Figure 11 compares the two different scenarios discussed above and presents one of the possible locations for the flashover in the half cycle of the AC voltage.

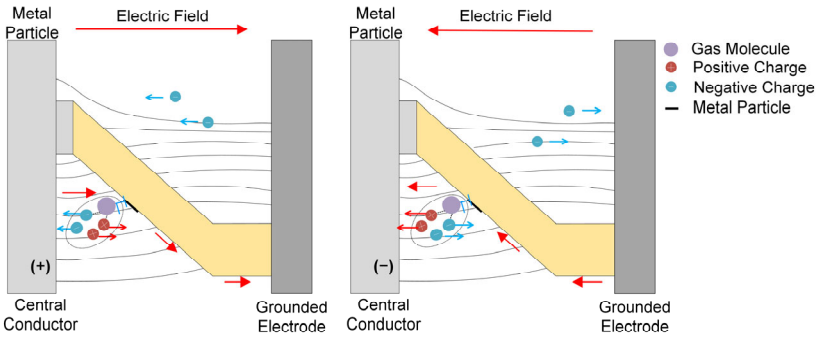


Figure 9. Mechanism of metal-particle-induced ionization and electric field enhancement.

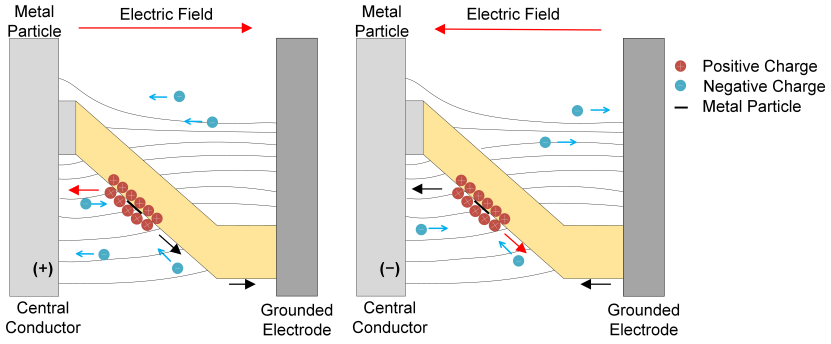


Figure 10. Effect of charge spot on gas ionization and electric field mitigation (marked in red and black arrows along the insulator surface).

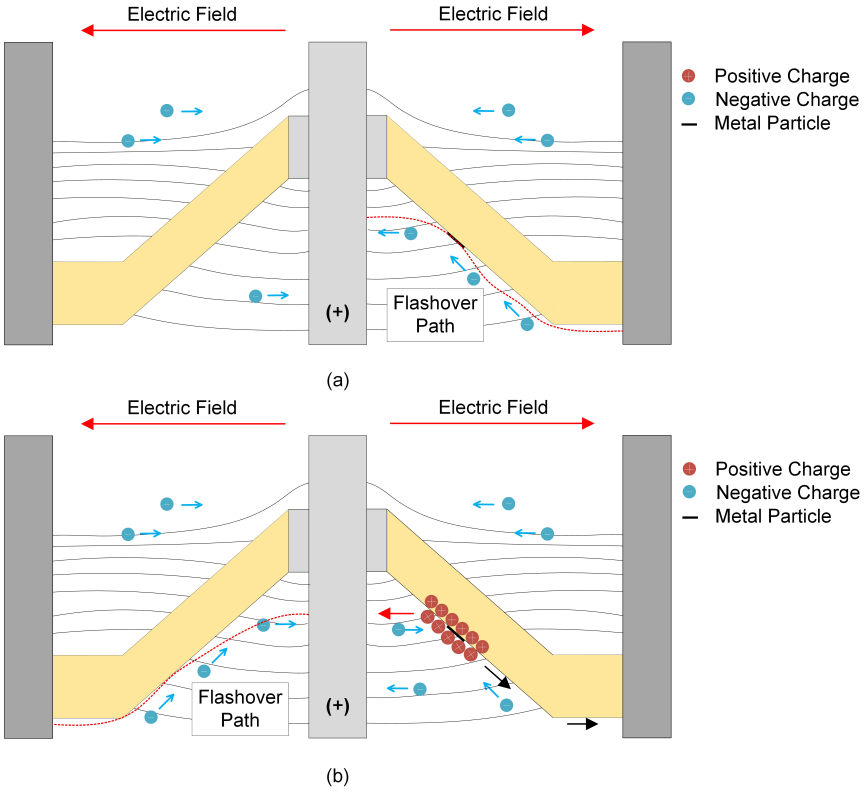


Figure 11. Effect of pre-charging on flashover paths: (**a**) without pre-charging; (**b**) with pre-charging.

When the metal particle is adhered to the grounded electrode area, negative charge spots are accumulated. During the positive half cycle, given the fact that the negative charge spot is accumulated away from the central conductor and the place where electrons collide with the insulator, the effect of the charge spot is relatively weak. In the negative half cycle, the metal particle and the negative charge spot mitigate the tangential electric field along the surface of the insulator as well. As a result, the electrical strength along the metal particle is increased, and the flashover occurs at other locations. In other words, the flashover voltages are increased, and the flashover arcs are 'driven away'.

5. Conclusions

In this article, the effect of the metal particle position and AC pre-charging on flashover properties of down-scaled basin insulators in C_4F_7N/CO_2 mixtures has been investigated, and the main conclusions can be summarized as follows.

1. Without pre-charging, the metal particle will decrease the flashover voltage when attached to the HV electrode and the middle area of the insulator. The attachment to the HV electrode of the insulator has a more pronounced effect on the flashover voltage than the middle area, and the attachment to the concave surface is more dangerous than the convex surface.
2. After a 5 min procedure of pre-charging, the flashover voltage of the sample, adhered with a metal particle, rises to nearly the same level as the instance of no metal particle adhered.
3. Carbonized burnt traces are left on the concave surface of the sample during the flashover, and the traces are distributed randomly when the metal particle is on the convex surface. When the metal particle is on the concave surface, the flashover occurs through the metal particles, but after pre-charging, the flashover arcs are driven away from the metal particle.

In short, it is found that the metal particle will decrease the flashover voltage when attached to the HV electrode and the middle area of the insulator. Surface charge will act synergistically with the metal particle, increasing the flashover voltage and redirecting the arc. Such findings deepen the understanding of flashover properties on epoxy insulators under AC voltage and provide valuable information for the selection of eco-friendly choices loaded in GIS, and offer references for the operation of environmentally friendly GIS.

Author Contributions: Conceptualization, J.G. and Y.G.; methodology, J.G. and Y.G.; software, Q.S.; validation, G.H., X.Q. and Y.G.; formal analysis, J.G., G.H. and Q.S.; investigation, J.G., G.H., Q.S. and X.Q.; resources, Y.G.; data curation, Q.S.; writing—original draft preparation, J.G. and Q.S.; writing—review and editing, X.Q., Z.W. and Y.G.; visualization, Q.S. and X.Q.; supervision, Y.G.; project administration, Z.W.; funding acquisition, Z.W. All authors have read and agreed to the published version of the manuscript.

Funding: This work is financially supported by China Electrical Equipment Group Co., Ltd. (CEE-2023-B-01-01-008-XD).

Data Availability Statement: The original contributions presented in this study are included in the article. Further inquiries can be directed to the corresponding author.

Conflicts of Interest: Author Jian Guan, Guohui Han, Xiaohu Qi, and Zhiying Wang are employed by the company HENAN PINGGAO ELECTRIC CO., LTD. The remaining authors declare that the research was conducted in the absence of any commercial or financial relationships that could be construed as a potential conflict of interest. The authors declare that this study received funding from China Electrical Equipment Group Co., Ltd. (CEE-2023-B-01-01-008-XD). The funder was not involved in the study design, collection, analysis, interpretation of data, the writing of this article or the decision to submit it for publication.

References

1. Okubo, H.; Beroual, A. Recent trend and future perspectives in electrical insulation techniques in relation to sulfur hexafluoride (SF6) substitutes for high voltage electric power equipment. *IEEE Electr. Insul. Mag.* **2011**, *27*, 34–42. [CrossRef]
2. Eriksson, A.; Pettersson, K.G.; Krenicky, A.; Baker, R.; Ochoa, J.R.; Leibold, A. Experience with gas insulated substations in the USA. *IEEE Trans. Power Deliv.* **1995**, *10*, 210–218. [CrossRef]
3. Riechert, U.; Holaus, W. Ultra high-voltage gas-insulated switchgear—A technology milestone. *Eur. Trans. Electr. Power* **2012**, *22*, 60–82. [CrossRef]
4. Zhang, X.; Li, G.; Huang, R.; Xiang, Z.; Zhang, Y.; Yao, S.; Wang, X. Statistical analysis of defects and maintenance advice for GIS in different operating years above 110 kV. *High-Volt. Electr. Appl.* **2016**, *52*, 184–188+194. [CrossRef]
5. Peng, P.; Ren, P.; Li, Q. Calculation method of thermal decomposition kinetic parameters of basin-type insulators in GIS. *High Volt. Eng.* **2020**, *46*, 3622–3629.
6. Li, C.; Lin, C.; Yang, Y.; Zhang, B.; Liu, W.; Li, Q.; Hu, J.; He, S.; Liu, X.; He, J. Novel HVDC spacers by adaptively controlling surface charges—Part ii: Experiment. *IEEE Trans. Dielectr. Electr. Insul.* **2018**, *25*, 1248–1258. [CrossRef]
7. Xie, J.; Chalmers, I.D. The influence of surface charge upon flash-over of particle-contaminated insulators in under impulse-voltage conditions. *J. Phys. D Appl. Phys.* **1997**, *30*, 1055. [CrossRef]
8. Winter, A.; Kindersberger, J. Surface charge accumulation on insulating plates in SF/sub 6/ and the effect on DC and AC breakdown voltage of electrode arrangements. In Proceedings of the Annual Report Conference on Electrical Insulation and Dielectric Phenomena, Cancun, Mexico, 20–24 October 2002; pp. 757–761.
9. Yanqin, L.; Guangning, W.; Guoqiang, G.; Jianyi, X.; Yongqiang, K.; Chaoqun, S. Surface charge accumulation behavior and its influence on surface flashover performance of Al_2O_3-filled epoxy resin insulators under DC voltages. *Plasma Sci. Technol.* **2019**, *21*, 055501.
10. Xie, Q.; Liang, S.; Fu, K.; Liu, L.; Huang, H.; Lü, F. Distribution of polymer surface charge under DC voltag and its influence on surface flashover characteristics. *IEEE Trans. Dielectr. Electr. Insul.* **2018**, *25*, 2157–2168. [CrossRef]
11. Kieffel, Y.; Biquez, F.; Vigouroux, D.; Ponchon, P.; Schlernitzauer, A.; Magous, R.; Cros, G.; Owens, J.G. Characteristics of g^3—An alternative to SF6. *CIRED* **2017**, *2017*, 54–57. [CrossRef]
12. Li, Z.; Ding, W.; Liu, Y.; Li, Y.; Zheng, Z.; Liu, W.; Gao, K. Surface flashover characteristics of epoxy insulator in C_4F_7N/CO_2 mixtures in a uniform field under AC voltage. *IEEE Trans. Dielectr. Electr. Insul.* **2019**, *26*, 1065–1072. [CrossRef]
13. Li, Z.; Zheng, Z.; Liu, Y.; Ding, W.; Li, X. Surface flashover characteristics of the 252 kV conical insulator in C_4F_7N/CO_2 gas mixtures under AC voltage. *Trans. China Electrotech. Soc.* **2020**, *35*, 62–69.
14. Gao, Y.; Wang, H.; Yuan, X.; Zhao, H.; Li, Z. Surface Charge Accumulation on a Real Size Epoxy Insulator with Bouncing Metal Particle Under DC Voltage. *IEEE Trans. Plasma Sci.* **2021**, *49*, 2166–2175. [CrossRef]
15. Morcos, M.M.; Zhang, S.; Srivastava, K.D.; Gubanski, S.M. Dynamics of metallic particle contaminants in GIS with dielectric-coated electrodes. *IEEE Trans. Power Deliv.* **2000**, *15*, 455–460. [CrossRef]
16. Li, S.; Gao, Y.; Lu, D.; Huang, P.; Du, B. Phase Dependence of Surface Charge Measurement on Epoxy Insulator in C_4F_7N/CO_2 under AC Voltage. *Polymers* **2024**, *16*, 2585. [CrossRef] [PubMed]
17. Wu, S.; Xu, H.; Zhang, X.; Liang, Y.; Shao, Y.; Wang, C.; Tu, Y.; Xu, Y. Towards the surface flashover in DC GIL/GIS: The electric field distribution and the surface charge accumulation. *Phys. Scr.* **2022**, *97*, 072001. [CrossRef]
18. Li, Z.; Liu, J.; Ohki, Y.; Chen, G.; Li, S. Surface flashover in 50 years: II. Material modification, structure optimisation, and characteristics enhancement. *High Volt.* **2025**, *10*, 243–278. [CrossRef]
19. Mustata, F.; Tudorachi, N. Thermal behavior of epoxy resin cured with aromatic dicarboxylic acids. *J. Therm. Anal. Calorim.* **2016**, *125*, 97–110. [CrossRef]
20. Zhong, L.; Hu, Y.; Qu, Z.; Tang, N.; Wang, F.; Du, J.; Li, L.; Chen, S.; Sun, Q. Solid Product Analysis on the Epoxy Resin Surface After Flashovers in C_4F_7N-Based Gas Mixtures Under Negative DC Voltage. *IEEE Trans. Dielectr. Electr. Insul.* **2024**, *31*, 246–253. [CrossRef]

Disclaimer/Publisher's Note: The statements, opinions and data contained in all publications are solely those of the individual author(s) and contributor(s) and not of MDPI and/or the editor(s). MDPI and/or the editor(s) disclaim responsibility for any injury to people or property resulting from any ideas, methods, instructions or products referred to in the content.